

Research Article

Mathematical Strategies for Design Optimization of Multiphase Materials

Rick Catania, Abdalla Diraz, Dominic Maier, Armani Tagle, and Pinar Acar 

Department of Mechanical Engineering, Virginia Tech, Blacksburg, VA 24061, USA

Correspondence should be addressed to Pinar Acar; pacar@vt.edu

Received 18 December 2018; Revised 12 February 2019; Accepted 21 February 2019; Published 12 March 2019

Academic Editor: R. Emre Erkmén

Copyright © 2019 Rick Catania et al. This is an open access article distributed under the Creative Commons Attribution License, which permits unrestricted use, distribution, and reproduction in any medium, provided the original work is properly cited.

This work addresses various mathematical solution strategies adapted for design optimization of multiphase materials. The goal is to improve the structural performance by optimizing the distribution of multiple phases that constitute the material. Examples include the optimization of multiphase materials and composites with spatially varying fiber paths using a finite element analysis scheme. In the first application, the phase distribution of a two-phase material is optimized to improve the structural performance. A radial basis function (RBF) based machine learning algorithm is utilized to perform a computationally efficient design optimization and it is found to provide equivalent results with the physical model. The second application concentrates on the optimization of spatially varying fiber paths of a composite material. The fiber paths are described by the Non-Uniform Rational Bezier (B)-Spline Surface (NURBS) using a bidirectional control point representation including 25 parameters. The optimum fiber path is obtained for various loading configurations by optimizing the NURBS parameters that control the overall distribution of fibers. Next, a direct sensitivity analysis is conducted to choose the critical set of parameters from the design point to improve the computational time efficiency. The optimized fiber path obtained with the reduced number of NURBS parameters is found to provide similar structural properties compared to the optimized fiber path that is modeled with a full NURBS representation with 25 parameters.

1. Introduction

As we move towards a new era for the design of high-performance materials, computational techniques utilizing emerging mathematical concepts become more crucial. The present work focuses on different mathematical approaches including gradient-based optimization, sensitivity analysis, and machine learning algorithms which are implemented into the design optimization of multiphase materials. The mathematical techniques are exercised first for the design of a composite material, which is made of two different material phases, where one is significantly softer than the other. The multiphase material reflects the nature's capability of producing multiple phases with complementary properties. By designing the material, our goal is to find the optimum distribution of the soft phase to avoid large stress concentrations in the structure. The design optimization is first performed using a finite element model, and the optimum element numbers that are made of the soft material phase are identified by minimizing the maximum von Mises stress. Next, a radial basis function (RBF) network based machine

learning algorithm is utilized using the samples generated with the finite element model to achieve a predictive model of the von Mises stress in terms of the soft material element numbers. The "machine learning" paradigm has recently gained a lot of interest from materials modeling and design communities [1–5] since it enables the integration of mathematical techniques/data science tools with the experiments and/or physical models. The computational material models are limited by the time constraints, experimental conditions, or theoretical foundations. Therefore, the machine learning algorithms have been recognized as a computationally efficient alternative to accelerate the modeling and design of materials [6, 7]. The basic principle of the machine learning algorithms depends on the mapping between the fingerprints and target properties. The machine learning techniques have recently been exercised to study the design of 3D printed composites involving multiple phases to improve the mechanical performance of materials [8, 9]. Although these previous studies presented a more rigorous mechanical problem in terms of the number of design variables and complexity of the objectives, the goal of the present work is

to implement different mathematical strategies for composite materials design for different problem types. One strategy is based on the RBF approach, which is introduced in this work as a machine learning algorithm that can be utilized to design multiphase materials. The RBF network model that is studied in this work is actually a type of artificial neural network model for application to problems of supervised learning [10]. In the RBF framework, the input variables are assigned to be the soft element numbers, the hidden layers are defined using a Gaussian function, and the output variable is determined as the maximum von Mises stress to be minimized. The RBF network leads to a more computationally efficient optimization and provides an identical solution compared to the optimum solution that is obtained using the finite element model. The presented design optimization scheme with the RBF network shows a preliminary study that can be adapted in the future to the more complicated design optimization studies for the composite materials utilizing a denser finite element mesh.

The second application concentrates on the optimization of the fiber paths of a composite lamina with a cutout at its center. Our goal is first to minimize the stress concentrations around the cutout and then to solve the design problem with a more computationally efficient strategy. The optimization of composite fiber paths has been a long-standing computational problem to improve the desired material performance without geometric changes [11–14]. The fiber path optimization is also closely related to the manufacturing of the composite materials that have spatially varying fiber distributions. Automated Fiber Placement (AFP) has been recognized as a leading manufacturing technique owing to the ability to reduce the waste and increase the deposition rate as opposed to the hand lay-up [15, 16]. On the other hand, the plate with a cutout is a well-known design problem in engineering mechanics. The first known closed-form theoretical solution was proposed by Kirsch [17] to compute the stress concentrations around cutouts of an infinite lamina under uniaxial tension. Notable studies in this field include many other applications that followed Kirsch's work later. For example, Mansfield [18] studied the stress state of an isotropic plate with a cutout to reduce the stress concentrations. Tang [19] studied the interlaminar stresses in orthotropic plates. The uniaxial tensile loading problem was studied by Senocak and Waas [20, 21] to reduce the stress concentrations around the cutout. Other prevalent studies include the finite element solver developed by Tatting and Gurdal [22, 23] to analyze elastically tailored composite materials and different design techniques that have been presented in [15, 24–27] to optimize spatially varying fiber paths. The finite element analysis is a popular technique to model the mechanical properties of the steered fiber composites [22, 23, 28–38]. The finite element modeling is also utilized in the present work to compute the stress concentrations around the cutout of a composite lamina. The Non-Uniform Rational Bezier (B)-Spline Surface (NURBS) [39] is implemented to describe the fiber path distribution. The NURBS uses Bezier splines (B-splines) to define the fiber path distributions. The goal is to obtain the optimum fiber path distribution for the composite lamina that minimizes

the maximum von Mises stress value. First, the NURBS representation is integrated into the finite element solver, and the NURBS parameters that describe the optimum fiber path are identified. For a high-fidelity representation of the fiber paths, we used 25 NURBS parameters (5×5 shape matrix) to control the fiber distribution. However, it also means that the optimization is performed to find the optimum values of all these 25 parameters, which leads to a computationally expensive problem. To improve the computational efficiency, we perform a direct sensitivity study to eliminate the less sensitive set of parameters from the optimization problem and, finally, reduce the number of optimization variables from 25 to 8. Using the sensitive parameters (8 parameters), the optimization is performed again and a similar optimum solution is obtained by decreasing the computational time requirement significantly. The solution strategy shows a preliminary case study that can be studied in the future for design optimization of spatially varying fiber paths under the effects of manufacturing uncertainties. The organization of the paper is as follows: Section 2 explains the finite element model for both application problems. Section 3 discusses the optimization of the multiphase material using finite element modeling and RBF based machine learning strategy. Section 4 addresses the fiber path optimization of a composite lamina with a cutout using the full and reduced sets of NURBS parameters. A summary and a discussion of the potential extensions as a future work are presented in Section 5.

2. Finite Element Model

The multiphase materials are analyzed with a finite element scheme in this work. The modeling approaches differ for the multiphase material and the composite with spatially varying fiber paths. In this section, we discuss the fundamental principles behind the finite element modeling for both cases.

2.1. Finite Element Modeling of Composite Materials. The finite element modeling of the composite material is based on the use of the two-dimensional quadrilateral elements. The material is assumed to include two phases: a stiff phase and a soft phase. Both phases are assumed to be isotropic. The stiff phase has a Young's modulus value of $E = 1000$ GPa and a Poisson's ratio of $\nu = 0.3$. The Young's modulus and Poisson's ratio values are as follows for the soft phase: $E = 100$ GPa and $\nu = 0.3$. For this preliminary application, the material is modeled using 16 quadrilateral elements, where each element can be made of either soft or stiff phase. We assume that 25% of the material (4 finite elements) should be made of the soft phase and then solve an optimization problem to identify the element numbers that should be made of the soft phase for better mechanical performance. We consider that the material is fixed at one side and it is under the effect of tensile loading (the stress is defined as $T_x = 1$ MPa) as shown in Figure 1.

2.2. Finite Element Modeling of Composite Materials with Spatially Varying Fiber Paths. For modeling the spatially varying fibers, the finite element is based on the constitutive

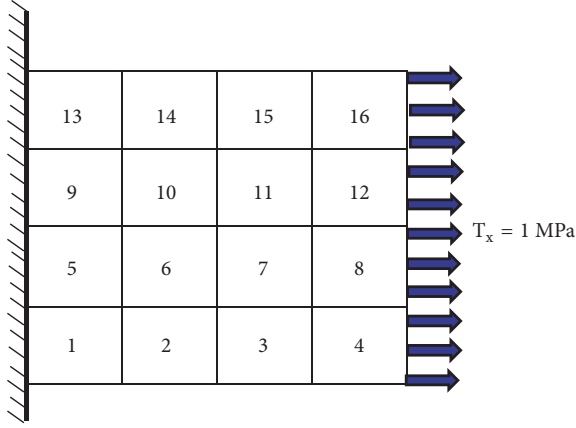


FIGURE 1: Representation of the problem geometry and finite element mesh. The problem is modeled with 16 quadrilateral finite elements, where each element can be made of either a soft or stiff phase.

matrix that is computed in the global frame, Q_{ij} (where $i, j = 1, 2, 3, 4, 5, 6$). However, the problem needs to be assembled and solved in the material frame. Therefore, the constitutive matrix of the material frame, \overline{Q}_{ij} , is calculated for each finite element using the transformation through the fiber angles, defined as θ . For a three-dimensional orthotropic material, the stress-strain equation can be defined as follows in the global solution frame:

$$\begin{bmatrix} \sigma_{xx} \\ \sigma_{yy} \\ \sigma_{zz} \\ \sigma_{zx} \\ \sigma_{yz} \\ \tau_{xy} \end{bmatrix} = \begin{bmatrix} Q_{11} & Q_{12} & Q_{13} & 0 & 0 & 0 \\ Q_{12} & Q_{22} & Q_{23} & 0 & 0 & 0 \\ Q_{13} & Q_{23} & Q_{33} & 0 & 0 & 0 \\ 0 & 0 & 0 & Q_{44} & 0 & 0 \\ 0 & 0 & 0 & 0 & Q_{55} & 0 \\ 0 & 0 & 0 & 0 & 0 & Q_{66} \end{bmatrix} \begin{bmatrix} \epsilon_{xx} \\ \epsilon_{yy} \\ \epsilon_{zz} \\ \gamma_{zx} \\ \gamma_{yz} \\ \gamma_{xy} \end{bmatrix} \quad (1)$$

where the stiffness coefficients (Q_{ij} values) are dependent on the orthotropic material properties E_{11} , E_{22} , ν_{12} , ν_{23} , and G_{23} . Next, the transformation matrix, $[L] = L(\theta)$, can be found as follows for each finite element:

$$[L] = \begin{bmatrix} 1 & 0 & 0 & 0 & 0 & 0 \\ 0 & c^2 & s^2 & 2c_p s_p & 0 & 0 \\ 0 & s^2 & c^2 & -2C_p s_p & 0 & 0 \\ 0 & -c_p s_p & c_p s_p & c_p^2 - s_p^2 & 0 & 0 \\ 0 & 0 & 0 & 0 & c_p & -s_p \\ 0 & 0 & 0 & 0 & s_p & c_p \end{bmatrix} \quad (2)$$

where $c_p = \cos(\theta)$ and $s_p = \sin(\theta)$ for each element “ m ”. The constitutive matrix in the material frame is found with the transformation as $\overline{Q} = [L]^T [Q] [L]$. The design optimization for the spatially varying fiber paths is demonstrated for several problems including different loading configurations (tensile and shear forces) and boundary conditions. Each

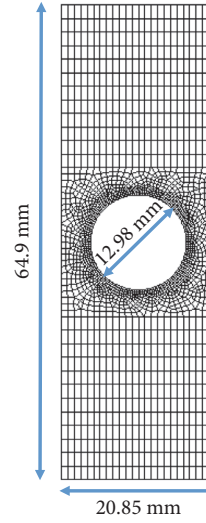


FIGURE 2: Representation of the problem geometry and the finite element mesh. The problem is modeled using 2019 quadrilateral elements. The finite element mesh is denser around the cutout, since the stress concentrations are expected to be higher.

problem is modeled using 2019 quadrilateral finite elements as shown in the problem geometry in Figure 2. The finite element mesh is denser around the cutout (Figure 2), since the stress concentrations are expected to be higher. More details on the finite element modeling of composite materials and derivation of the material matrices were discussed in the previous works [35–38] and they are not repeated in this work for brevity. The finite element library used in this study is an in-house code that is developed to model composite materials. The library has been previously validated against the theoretical results in our previous publications [35–38].

2.3. Representation of the Composite Fiber Path. The NURBS representation is mainly used as a mathematical model for generating curves/surfaces. In this approach, the shape of a curve is defined by a set of control points and thus it can describe a large variety of shapes. The fiber paths are defined as contours of the NURBS surface by assuming domain dimensions given in Figure 2. The choice for the order of control set points is critical, since they are correlated with the shape of the fiber path. In order to allow a smooth and continuous fiber path distribution and to increase the variability of the fiber paths, a bidirectional control point representation including 25 points on a 5×5 grid that are equally spaced in x and y directions is selected. This also means that the entire fiber path distribution of the composite material depends on these 25 parameters, and thus the fiber path distribution can be optimized by optimizing the NURBS parameters. Some of the generic fiber path distributions of a composite material are illustrated with the NURBS representation in Figure 3. More information on the mathematical background for the definition of the surfaces and curves using the NURBS representation can be found in [40].

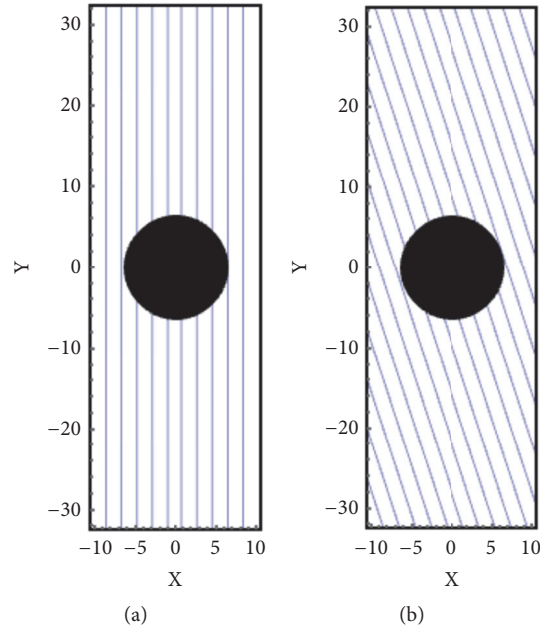


FIGURE 3: Fiber paths aligned at (a) 90° and (b) 45°.

3. Design Optimization of the Composite Material

In the first application, the design of a composite material that is made of soft and stiff material phases is discussed. Our goal is to minimize the stress concentrations and, thus, the design objective is defined as the minimization of the maximum von Mises stress of the structure. It is assumed that the 25% of the material is made of the soft phase. The problem is modeled using 16 quadrilateral finite elements (Figure 1). We aim to find the optimum distribution of the soft phase and, thus, the optimization variables are defined as the element numbers of the soft phase. The first solution includes the integration of the Sequential Quadratic Programming (SQP) optimization algorithm to the full finite element scheme. Next, we utilize the RBF as a machine learning algorithm to develop a predictive model of the maximum von Mises stress (design objective) in terms of the element numbers of the soft material phase (design variables). The SQP algorithm is used with the predictive model to find the optimized material distribution. The first part of this subsection discusses the optimization results that are obtained with the full finite element scheme, while the second subsection concentrates on the RBF definition and optimization with the machine learning approach.

3.1. Optimization with the Finite Element Model. The optimum material distribution problem (given in Figure 1) is identified with the SQP algorithm. The mathematical definition of the optimization problem is as follows:

$$\begin{aligned}
 & \min v_m^{max} \\
 & \text{subject to: } x_i - x_{i+1} \leq -1, \quad i = 1, 2, 3 \\
 & \quad x = (x_1, x_2, x_3, x_4) \in Z^n \\
 & \quad \text{where } 1 \leq x \leq 16
 \end{aligned} \tag{3}$$

In (3), the objective is defined as the minimization of the maximum von Mises stress, v_m^{max} . The optimization variables are the element numbers of the soft phase, which are denoted as x_1, x_2, x_3, x_4 , since there are 4 soft elements in the structure. The optimization variables are the subset of the integer solution space, Z^n , and the maximum value they can take is equal to the number of total finite elements (16 elements). Note that each optimization variable should also have a different integer value to find the optimum distribution. Therefore, the parameters are ordered by assuming the following relation: $x_1 < x_2 < x_3 < x_4$, and the corresponding design constraint, $x_i - x_{i+1} \leq -1$ (for $i = 1, 2, 3$), is introduced to the problem definition in (3). The problem is solved with the SQP algorithm, and the optimum material distribution is obtained as shown in Figure 4. The maximum von Mises stress value, v_m^{max} , of the optimum configuration is found as 135.61 kPa. The optimum solution provides an 88.05% decrease in maximum von Mises stress value compared to the maximum von Mises stress value (1134.4) kPa of the structure which is only made of the stiff phase. Note that the optimum design of this problem leads to a nonunique solution. Some of the multiple optimum solutions are symmetric, and the rest of the solutions are asymmetric (e.g., the optimum solution illustrated in Figure 4).

3.2. Optimization with the Machine Learning Model. The design optimization problem for the composite material is also solved with the implementation of a machine learning strategy. The RBF network is utilized for this purpose to model the integer optimization variables that define the element numbers of the soft phase as input parameters. The objective function variable, maximum von Mises stress (v_m^{max}), is assigned as the output variable. A general RBF consists of an input layer, hidden layer(s), and output layer as shown in Figure 5. The input layer stores the information for

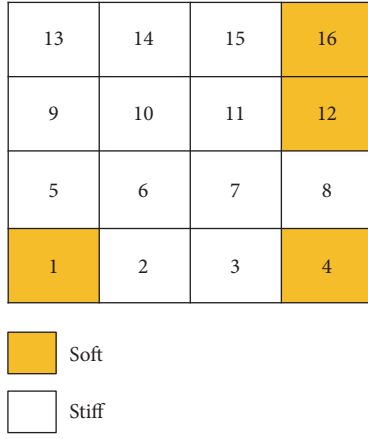


FIGURE 4: Optimum material phase distribution for the composite material design problem.

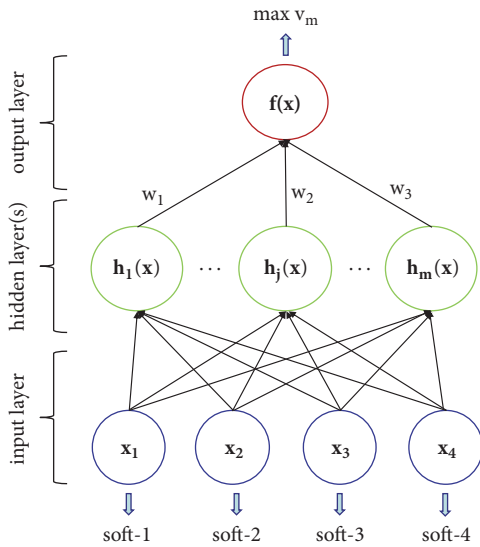


FIGURE 5: RBF network framework for the composite material design problem. The input layer consists of the element numbers of the soft elements (soft-1, soft-2, soft-3, and soft-4). The hidden layer contains the RBF transformation, and the output layer stores the information regarding the output variable, maximum von Mises stress.

the optimization variables, which are defined as the element numbers of the soft elements. Each of these four components of the input vector, \mathbf{x} , feeds the system information and forwards it to m basis functions on the hidden layer. Note that the RBF framework can include multiple hidden layers. The outputs of the basis functions (or the hidden layers in general) are linearly combined with the weights, w_j ($j = 1, 2, \dots, m$), into network output, $f(x)$. The output is defined as the objective function variable, which is the maximum von Mises stress.

The RBF network is used to predict the maximum von Mises stress value (output value) as a function of the soft element numbers (design variables). To generate the training dataset, we create 100 random design samples for soft element

numbers and store the corresponding maximum von Mises stress values. The accuracy of the prediction obtained with the RBF network is checked with the following minimization problem:

$$\min z = \sum \|Y_* - Y\| \quad (4)$$

where Y_* shows the RBF prediction of the output variable and Y is the output variable values for the random design samples. The minimization problem is solved to find the hyperparameters that define the RBFs in the hidden layers, given with a Gaussian function [10]:

$$h(\mathbf{x}) = \exp\left(\frac{-(\mathbf{x} - c)^2}{r^2}\right) \quad (5)$$

where c is the center and r is the radius of the Gaussian RBF. They are also called hyperparameters, and, in the present work, they are obtained by the SQP algorithm with the minimization problem in (4). The RBF network is generated using 25 hidden layers, and the corresponding min z value is found to be very small such that $z < 10^{-12}$. The design optimization for finding the optimum element numbers of the soft phase is repeated using the generated RBF network, and the same optimum solution shown in Figure 5 is obtained with the same maximum von Mises stress value. The optimization with the finite element and NN models is started with the same initial guess, and thus both cases converge to the same optimum solution.

4. Design Optimization of Composite Fiber Paths

4.1. *Optimization with the Finite Element Model.* In the second application, the finite element modeling scheme is utilized to design a composite material with a spatially varying fiber distribution. The fiber paths in a thin symmetrical lamina with a circular cutout are generated based on predefined boundary conditions. Traditionally, layers of laminates follow linear 90° and 45° angles (Figure 3). The new fiber placement around a circular cutout would ideally enhance the material's reaction to different stresses. The dimensions of the plate are assumed to be 64.9 mm by 20.85 mm by 1 mm, as well as a hole in the center with a diameter of 12.98 mm (Figure 2). The plate is made of carbon-epoxy composite, and the material properties of the carbon-epoxy are given in Table 1.

The NURBS representation is implemented into the finite element model to define the fiber distributions of the composite lamina. The goal is to optimize the material properties in response to different stresses and boundary conditions. The same objective function of minimizing the maximum von Mises stress is considered. The mathematical definition of the optimization problem is given as follows:

$$\min v_m^{max} \quad (6)$$

$$\mathbf{s} = [\boldsymbol{\beta}]$$

where \mathbf{s} shows the set of optimization variables, which are assigned as the NURBS shape parameters that are controlled

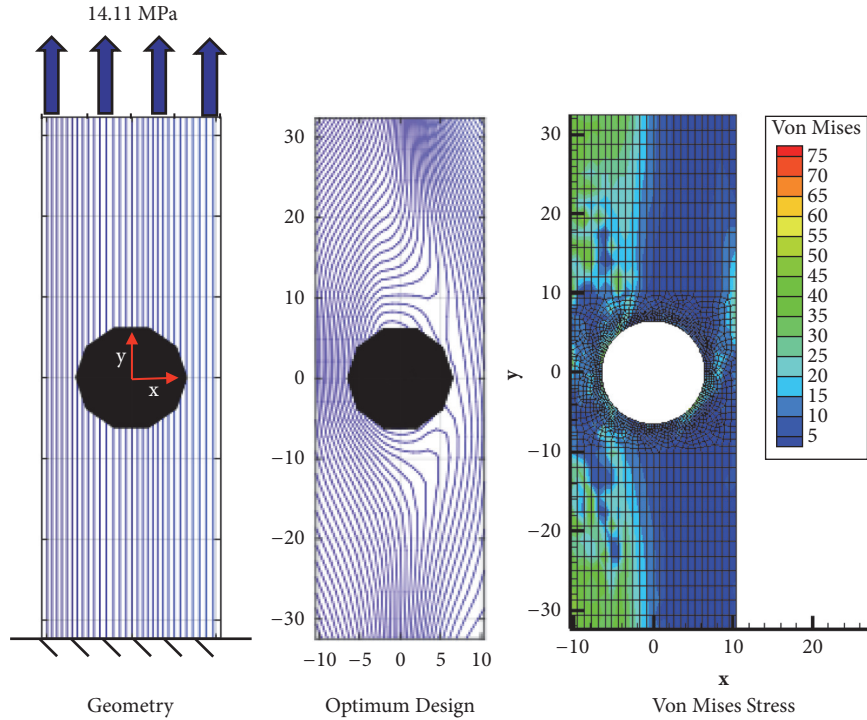


FIGURE 6: The geometry of the problem, optimum fiber path, and the von Mises stress distribution of the optimum design (Case-I). The minimum objective function is obtained as $v_m^{max} = 61.87$ MPa.

TABLE 1: Material properties of carbon-epoxy.

Property	Value
E_{xx}	145.880 GPa
E_{yy}	13.312 GPa
E_{zz}	13.312 GPa
G_{xy}	4.386 GPa
G_{xz}	4.386 GPa
G_{yz}	4.528 GPa
G_{xy}	4.386 GPa
ν_{xy}	0.263
ν_{xz}	0.470
ν_{yz}	0.470

by the 5×5 shape matrix, $[\beta]$. The optimization problem given in (6) is solved for the same plate subjected to three different cases of tensile and shear loading under different boundary conditions. The problem geometry, optimum fiber distributions, and the distributions of the von Mises stress in the optimum configurations are shown for each case in Figures 6, 7, and 8, respectively. Note that the geometric definition of the problem also shows our initial guess for the fiber path distribution that is taken as an input in the SQP optimization solver.

Case-I (Figure 6) focuses on a tensile loading problem for the rectangular plate that is fixed at the bottom. The optimum fiber path and the corresponding von Mises stress distributions are also shown in Figure 6. The problem in

Case-II (Figure 7) is also a tensile loading problem with different boundary conditions. The roller boundary conditions illustrated in Figure 7 lead to zero x -displacement on the left side and zero y -displacement on the right side. The last application (Case-III) is a shear loading problem, and the problem geometry, optimum fiber path, and the corresponding von Mises stress distributions are illustrated in Figure 8. Each of the optimization studies takes about 5.5 – 6 hours on the same computational platform. The computational cost is directly related to the number of design variables, which are the 25 NURBS parameters in this problem. However, some of the design variables may not be sensitive to the objective function. Therefore, elimination of these insensitive parameters should not only lead to a more computationally efficient optimization solution but also keep a similar accuracy level for the mechanical response. Our next goal is to reduce the problem size by eliminating less sensitive parameters in the optimization problem and to retain the accuracy of the optimum solution at the same time. To perform the sensitivity analysis, we generate random samples using a uniform probability distribution around the mean values of the NURBS parameters in our initial guess of the optimization problem. The parameters are assumed to vary $\pm 10\%$ around their initial values. The changes on the objective function are computed using these 100 random samples, and some of the NURBS parameters are found to be very insensitive to the von Mises stress value. Eight of the 25 NURBS parameters are found to be more sensitive to the von Mises stress, and thus the optimization study is performed again for Case-I (tensile loading acting on a

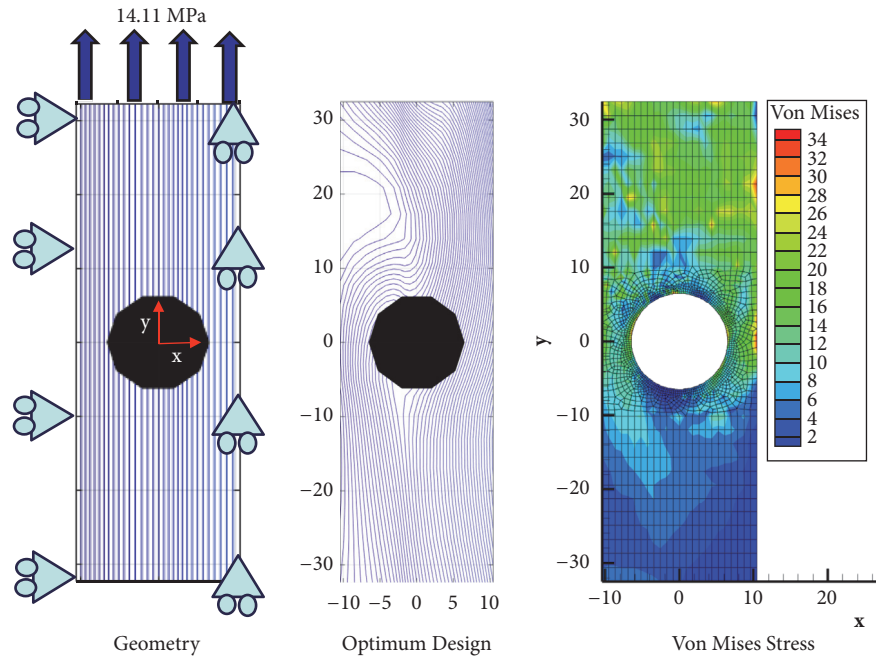


FIGURE 7: The geometry of the problem, optimum fiber path, and the von Mises stress distribution of the optimum design (Case-II). The minimum objective function is obtained as $v_m^{max} = 34.27$ MPa.

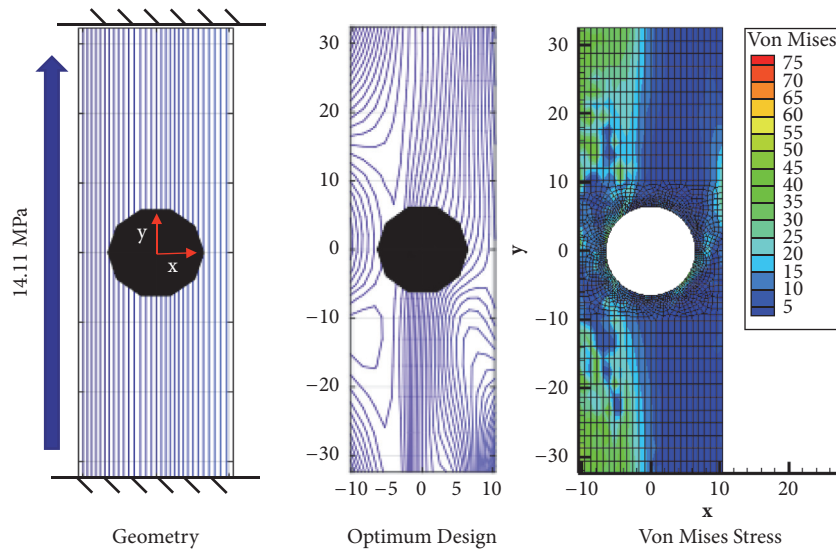


FIGURE 8: The geometry of the problem, optimum fiber path, and the von Mises stress distribution of the optimum design (Case-III). The minimum objective function is obtained as $v_m^{max} = 61.04$ MPa.

fixed plate) using these 8 parameters instead of the original 25 NURBS variables. The selected 8 parameters are the variables that can change the objective function value more than $\pm 0.5\%$ around its value for the initial guess design. The remaining parameters are assumed to have the initial guess values. The minimization problem gives a maximum von Mises stress value of 62.63 MPa, which is close to the optimum solution of the full problem (61.87 MPa) shown in Figure 6. The optimized fiber path and the corresponding von Mises stress distributions that are obtained using the 8

NURBS parameters are shown in Figure 9. The computational time required to solve the reduced problem with the SQP algorithm on the same computational platform is 1.1 hours, which is significantly less than the required time for the full problem (around 5.5–6 hours).

5. Conclusions

We present mathematical solution strategies that are applied to the computational design of multiphase materials. The first

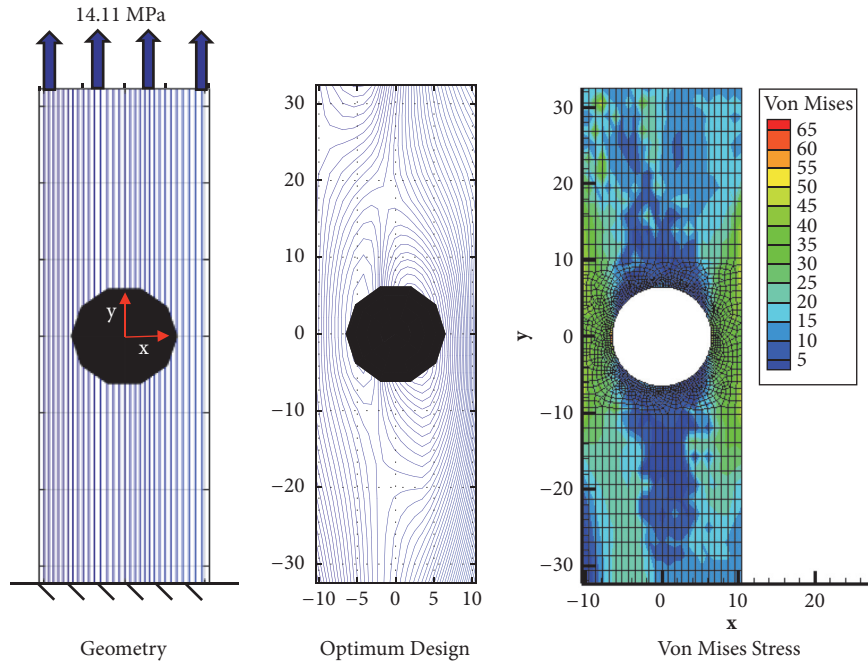


FIGURE 9: The optimum fiber path and the von Mises stress distribution of the optimum design for Case-I with reduced number of NURBS parameters. The minimum objective function is obtained as $v_m^{max} = 62.63$ MPa.

application focuses on the design of a composite material by finding the optimized distribution of the soft and stiff material phases. A finite element solution is utilized by assuming that each element is made of either the stiff or the soft phase, and the maximum von Mises stress is computed. Next, a radial basis function (RBF) network based machine learning algorithm is implemented into the finite element library to obtain a predictive model of the maximum von Mises stress value in terms of the element numbers of the soft material. The RBF approach is found to provide the same optimum material distribution with original finite element based modeling. In the second application, we aim to optimize the fiber path distribution of a composite plate having a cutout at its center. The fiber path distribution is described by the Non-Uniform Rational B-Spline Surface (NURBS) parameterization. In this representation, a 5×5 shape matrix including 25 independent NURBS parameters is used to control the fiber path. The optimum fiber distribution is obtained through optimizing the NURBS parameters to minimize the maximum von Mises stress. In the next step, less sensitive parameters are identified with a direct covariance computation through a sensitivity analysis, and they are eliminated from the optimization problem. The optimization is performed again for the remaining (more sensitive) NURBS parameters, and a similar minimum value for the objective function is obtained with better computational time efficiency. The studied mathematical techniques in this work present a preliminary design strategy for multi-phase materials. The future work may focus on the integration of the same techniques into more complex geometries and problems for stochastic design optimization of materials.

Nomenclature

ν :	Poisson's ratio
c :	Center of the RBF network
E :	Young's modulus
F :	Global force vector
h :	Hidden layer in the RBF network
K :	Global stiffness matrix
L :	Transformation matrix
\underline{Q} :	Constitutive matrix in the global frame
\overline{Q} :	Constitutive matrix in the material frame
r :	Radius of the RBF network
u :	Displacement
v_m^{max} :	Maximum von Mises stress
x :	Soft element numbers
Y_* :	RBF network prediction for the output
Y :	Output values in random design samples.

Data Availability

The data that support the findings of this study are available upon request from the corresponding author, Pınar Acar.

Disclosure

The research did not receive any specific funding. The institution it was performed at is "Virginia Polytechnic Institute and State University."

Conflicts of Interest

The authors declare that they have no conflicts of interest.

References

- [1] T. Mueller, A. G. Kusne, and R. Ramprasad, "Machine learning in materials science: recent progress and emerging applications," in *Reviews in Computational Chemistry*, pp. 186–273, John Wiley & Sons Inc, 2016.
- [2] L. Ward and C. Wolverton, "Atomistic calculations and materials informatics: a review," *Current Opinion in Solid State & Materials Science*, vol. 21, no. 3, pp. 167–176, 2017.
- [3] M. L. Green, C. L. Choi, J. R. Hattrick-Simpers et al., "Fulfilling the promise of the materials genome initiative with high-throughput experimental methodologies," *Applied Physics Reviews*, vol. 4, no. 1, Article ID 011105, 2017.
- [4] J. R. Hattrick-Simpers, J. M. Gregoire, and A. G. Kusne, "Perspective: Composition-structure-property mapping in high-throughput experiments: turning data into knowledge," *APL Materials*, vol. 4, no. 5, Article ID 053211, 2016.
- [5] R. Ramprasad, R. Batra, G. Pilania, A. Mannodi-Kanakkithodi, and C. Kim, "Machine learning in materials informatics: recent applications and prospects," *npj Computational Materials*, vol. 3, no. 54, 2017.
- [6] Y. Liu, T. Zhao, W. Ju, S. Shi, S. Shi, and S. Shi, "Materials discovery and design using machine learning," *Journal of Materiomics*, vol. 3, no. 3, pp. 159–177, 2017.
- [7] G. B. Olson, "Designing a new material world," *Science*, vol. 288, no. 5468, pp. 993–998, 2000.
- [8] G. X. Gu, L. Dimas, Z. Qin, and M. J. Buehler, "Optimization of composite fracture properties: method, validation, and applications," *Journal of Applied Mechanics*, vol. 83, no. 7, Article ID 071006, 2016.
- [9] G. X. Gu, S. Wettermark, and M. J. Buehler, "Algorithm-driven design of fracture resistant composite materials realized through additive manufacturing," *Additive Manufacturing*, vol. 17, pp. 47–54, 2017.
- [10] M. J. L. Orr, "Introduction to radial basis function networks," Technical Report, Institute for Adaptive and Neural Computation, Division of Informatics, Edinburgh University, Edinburgh, Scotland, UK, 1996, <http://www.anc.ed.ac.uk/mjo/rbf.html>.
- [11] Z. Gürdal and R. Olmedo, "Composite laminates with spatially varying fiber orientations: variable stiffness panel concept," in *Proceedings of the AIAA/ASME/ASCE/AHS/ASC 33rd Structures, Structural Dynamics and Materials Conference*, Dallas, TX, USA, 1992.
- [12] Z. Gürdal and R. Olmedo, "In-plane response of laminates with spatially varying fiber orientations: Variable stiffness concept," *AIAA Journal*, vol. 31, no. 4, pp. 751–758, 1993.
- [13] G. Raju, Z. Wu, B. C. Kim, and P. M. Weaver, "Prebuckling and buckling analysis of variable angle tow plates with general boundary conditions," *Composite Structures*, vol. 94, no. 9, pp. 2961–2970, 2012.
- [14] Z. Wu, P. M. Weaver, and G. Raju, "Postbuckling optimisation of variable angle tow composite plates," *Composite Structures*, vol. 103, pp. 34–42, 2013.
- [15] Z. Wu, P. M. Weaver, G. Raju, and B. Chul Kim, "Buckling analysis and optimisation of variable angle tow composite plates," *Thin-Walled Structures*, vol. 60, pp. 163–172, 2012.
- [16] D. H.-J. A. Lukaszewicz, C. Ward, and K. D. Potter, "The engineering aspects of automated prepreg layup: history, present and future," *Composites Part B: Engineering*, vol. 43, no. 3, pp. 997–1009, 2012.
- [17] G. Kirsch, "Die Theorie der Elastizität und die Bedürfnisse der Festigkeitslehre (in German) (The theory of elasticity and the needs of the Strength of Materials)," *Zeitschrift des Vereines Deutscher Ingenieure*, vol. 42, pp. 797–807, 1898.
- [18] E. H. Mansfield, "Neutral holes in plane sheet reinforced holes which are elastically equivalent to the uncut sheet," *The Quarterly Journal of Mechanics and Applied Mathematics*, vol. 3, pp. 370–378, 1953.
- [19] S. Tang, "Interlaminar stresses around circular cutouts in composite plates under tension," *AIAA Journal*, vol. 15, no. 11, pp. 1631–1637, 1977.
- [20] E. Senocak and A. Waas, "Design considerations for symmetrically laminated plates with cutouts," in *Proceedings of the 33rd Structures, Structural Dynamics and Materials Conference*, Dallas, TX, USA, 1992.
- [21] E. Senocak and A. M. Waas, "Neutrally reinforced holes in symmetrically laminated plates," *Journal of Aircraft*, vol. 30, no. 3, pp. 428–430, 1993.
- [22] B. F. Tatting and Z. Gürdal, "Design and manufacture of elastically tailored tow placed plates," NASA/CR-2002-211919, 2002.
- [23] B. F. Tatting and Z. Gürdal, "Automated finite element analysis of elastically-tailored plates," NASA/CR-2003-212679, 2003.
- [24] S. T. IJsselmuiden, M. M. Abdalla, S. Setoodeh, and Z. Gürdal, "Design of variable stiffness panels for maximum buckling load using lamination parameters," *AIAA Journal*, vol. 48, no. 1, pp. 134–143, 2010.
- [25] J. M. J. F. Van Campen, C. Kassapoglou, and Z. Gürdal, "Design of fiber-steered variable-stiffness laminates based on a given lamination parameters distribution," in *Proceedings of the 52nd AIAA/ASME/ASCE/AHS/ASC Structures, Structural Dynamics and Materials Conference*, Denver, Colo, USA, April 2011.
- [26] J. V. Risicato and X. Legrand, "Genetic algorithm used to optimize fiber steering in composite laminates," in *Recent Advances in Textile Composites*, pp. 26–28, France, Lille Grand Palais, Lille, France, 2010.
- [27] E. Lund, "Buckling topology optimization of laminated multi-material composite shell structures," *Composite Structures*, vol. 91, no. 2, pp. 158–167, 2009.
- [28] H. Ghasemi, R. Brighenti, X. Zhuang, J. Muthu, and T. Rabczuk, "Optimization of fiber distribution in fiber reinforced composite by using NURBS functions," *Computational Materials Science*, vol. 83, pp. 463–473, 2014.
- [29] S. Nagendra, S. Kodiyalam, J. E. Davis, and V. N. Parthasarathy, "Optimization of tow fiber paths for composite design," in *Proceedings of the 36th AIAA/ASME/ASCE/AHS/ASC Structures, Structural Dynamics, and Materials Conference and AIAA/ASME Adaptive Structures Forum. Part 1 (of 5)*, pp. 1031–1041, New Orleans, La, USA, April 1995.
- [30] A. V. Duran, N. A. Fasanella, V. Sundararaghavan, and A. M. Waas, "Thermal buckling of composite plates with spatial varying fiber orientations," *Composite Structures*, vol. 124, pp. 228–235, 2015.
- [31] A. V. Duran, N. A. Fasanella, V. Sundararaghavan, and A. M. Waas, "Optimization of composite plates with spatially varying fiber paths for thermal buckling," in *Proceedings of the 56th AIAA/ASCE/AHS/ASC Structures, Structural Dynamics, and Materials Conference 2015*, Kissimmee, Fla, USA, January 2015.
- [32] C.-C. Lin and C.-S. Kuo, "Buckling of Laminated Plates with Holes," *Journal of Composite Materials*, vol. 23, no. 6, pp. 536–553, 1989.
- [33] U. Topal and Ü. Uzman, "Maximization of buckling load of laminated composite plates with central circular holes using

- MFD method,” *Structural and Multidisciplinary Optimization*, vol. 35, no. 2, pp. 131–139, 2008.
- [34] H. Ounis, A. Tati, and A. Benchabane, “Thermal buckling behavior of laminated composite plates: a finite-element study,” *Frontiers of Mechanical Engineering*, vol. 9, no. 1, pp. 41–49, 2014.
- [35] P. Acar, A. A. Vijayachandran, V. Sundararaghavan, and A. M. Waas, “Fiber path optimization of a symmetric laminate with a cutout for thermal buckling,” *Journal of Aircraft*, vol. 54, no. 1, pp. 54–61, 2017.
- [36] P. Acar, A. A. Vijayachandran, V. Sundararaghavan, A. Waas, and M. Rassaian, “Optimization of spatially varying fiber paths for a symmetric laminate with a circular cutout under remote uniaxial tension,” *SAE Aerotech Congress and Exhibition*, vol. 9, no. 1, pp. 22–24, 2015.
- [37] P. Acar, A. A. Vijayachandran, V. Sundararaghavan, A. Waas, and M. Rassaian, “Optimization of spatially varying fiber paths for a symmetric laminate with a circular cutout under remote uniaxial tension,” *SAE International Journal of Materials and Manufacturing*, vol. 9, no. 1, pp. 75–80, 2016.
- [38] A. A. Vijayachandran, P. Acar, V. Sundararaghavan, and A. M. Waas, “Fiber path optimization of a composite plate with a cutout for thermal buckling,” in *Proceedings of the 57th AIAA/ASCE/AHS/ASC Structures, Structural Dynamics, and Materials Conference, 2016*, pp. 4–8, San Diego, Calif, USA, January 2016.
- [39] D. M. Spink, “NURBS matlab toolbox,” 2018, <https://www.mathworks.com/matlabcentral/fileexchange/26390-nurbs-toolbox-by-d-m-spink>.
- [40] L. Piegl and W. Tiller, *The NURBS Book*, Springer Science & Business Media, 2012.